

Synthesis of Mg-Ferrite nanoparticles via auto combustion method and investigation their structural, morphological and magnetic properties

Ibrahim F. Waheed , Faiz M. AL-Abady , Baidaa M. Ali

Department of Chemistry , College of Science , Tikrit University , Tikrit , Iraq

<https://doi.org/10.25130/tjps.v24i7.458>

ARTICLE INFO.

Article history:

-Received: 22 / 6 / 2019

-Accepted: 23 / 9 / 2019

-Available online: / / 2019

Keywords: Spinel structure; Sol-gel auto-combustion; Magnesium ferrite.

Corresponding Author:

Name: Ibrahim F. Waheed

E-mail: imaofs76@yahoo.com

Tel:

ABSTRACT

Magnesium ferrite ($MgFe_2O_4$) nanoparticles is prepared by sol-gel auto combustion method and calcinated at (200,450, 900) °C. The capping agent was urea and ($Mg(NO_3)_2 \cdot 6H_2O$) and ($Fe(NO_3)_3 \cdot 9H_2O$) nitrates as sources of metal. X-ray diffraction (XRD) and Fourier transform infrared spectroscopy (FT-IR) characteristic show clear modes of the cubic Mg-ferrite structure formation. Infrared spectrum of metal-oxygen vibration at (703-636) and (574-433) cm^{-1} show the tetrahedral and octahedral site of Mg-ferrite structure. Scanning Electron Microscope (SEM) images shown pure crystalline microstructure with polyhedral shapes and very small numbers of globular small particles. The crystallite size of Mg-ferrite is calculated using Debye-Scherrer relation and was in the range of 29 nm.

1. Introduction

The ceramic powder is generally known as ferrite could afford more features over the bulk ferrite with the suggestive change of physical properties like very tiny size and increasing the surface area [1,2]. Spinel ferrites crystals have chemical formula MFe_2O_4 , where M is Mn^{2+} , Co^{2+} , Ba^{2+} , Zn^{2+} , Cd^{2+} , Ni^{2+} , Mg^{2+} , Cu^{2+} , etc.) [3], The structure of spinel is determined by bonding and arrangement of the oxygen ions (O^{2-}) within the lattice points. The unit cell of a spinel lattice contains eight formula units $[(A)(B)_2O_4]$. The large oxygen anions (32 from O^{2-}) form a close-packed FCC structure. Whereas the few metal cations occupy interstitial sites: tetrahedral (8) or (A) and octahedral (16) or (B) sites. Depending on how cations occupy diverse interstices, a spinel structure can be categorized into normal or inverse. In the normal spinel, the tetrahedral voids are occupied by only the divalent (A^{+2}) ions whereas the octahedral voids are occupied by the trivalent (B^{+3}) ions only. These compounds shows lowly magnetic properties, for Example of normal spinel; $ZnFe_2O_4$, $CdFe_2O_4$, and $MgAl_2O_4$. On the other hand, inverse spinel, (A^{+2}) ions occupy the octahedral voids, whereas half of (B^{+3}) ions occupy the tetrahedral voids. It can be represented as $[(B^{+3})_{tet}(A^{+2}B^{+3})_{oct}O_4]$. $NiFe_2O_4$, Fe_3O_4 , and $CoFe_2O_4$ are classified under this group [4-6]. Among the known magnetic nanoparticles, magnesium ferrite, $MgFe_2O_4$, a well-known soft magnetic, n-type semiconductor [7], So it has much application such as heterogeneous catalysis,

photoelectrical, sensors, and magnetic technologies [8-16]. Conventionally, $MgFe_2O_4$ is usually synthesized by sol-gel auto combustion method [17-20], thermal treatment [21], coprecipitation method [22], hydrothermal synthesis [23], high energy ball milling [24] and spray pyrolysis [25], have been extensively investigated for the synthesis of well-dispersed $MgFe_2O_4$ nanoparticles. The methods refer to as have specific advantages dependent on required applications and properties of synthesized materials. The sol-gel auto-combustion technique has arisen as an essential processes for preparation of high-performance ceramics, catalysts, composites, and crystalline spinel oxide materials. In this technique, the chemical reaction is the exothermicity, used to synthesis useful compounds with homogeneous mixing, regular shape, and fine stoichiometric control [26-31]. The aim of the current study graft is to consider the plain structural and magnetic belongings of $MgFe_2O_4$ nanoparticles prepared via the auto combustion method with urea as fuel. The structure and morphology of the nanoparticles are characterized and analyzed by X-ray diffraction patterns, scanning electron microscopy and transmission electron microscopy. The magnetic properties for the $MgFe_2O_4$ nanoparticles, also, are measured by using vibrating sample magnetometer at room temperature.

2. Materials and Methods

Initial materials utilized in the existent work were: magnesium nitrate, CDH, 99%), ferric nitrate 9-hydrate ($\text{Fe}(\text{NO}_3)_3 \cdot 9\text{H}_2\text{O}$, CDH, 99.9%), urea ($\text{CO}(\text{NH}_2)_2$, CDH, 99.9%), and ammonium hydroxide (NH_4OH , Fluka). All chemicals in this work, were of analytical reagent grade. Deionized water is used in all the experiments.

2.1. Synthesis of magnetic nanospinel MgFe_2O_4

Mg-ferrite powder was combined affording to identified auto-combustion routes with revisions. The molar ratio of urea to metal ions (OH/M) is 2:1, while the molar ratio of Mg:Fe was specific to 1:2. In a distinctive method, known attention solutions of nitrate were equipped by dissolving $\text{Mg}(\text{NO}_3)_2 \cdot 6\text{H}_2\text{O}$, and $\text{Fe}(\text{NO}_3)_3 \cdot 9\text{H}_2\text{O}$ in the deionized water. solutions of nitrate were then variegated via volume agreeing for identified magnitudes and apposite weight of fuel (urea) lastly additional at the variegated mixture. The pH of the mixture was attuned at 8. after that the solution was heated at about 90°C under constant stirring, for 2h pending a gelatinous sol was attained. The gelatinous sol was animated on a hot plate about 100°C . The gel begins swelling, and then a quick and strong auto-ignition occurs for about a minute, finishing the reaction. the sample was heated in a furnace at 200°C for 2 h. The equipped powder was annealed in 450°C - 900°C for 2 h in air.

2.2. Characterization

The structural characterization of the manufactuerd compounds are Personalized by "Shemadzu X ray diffractometer (model 6000)". The period and crystallite size were examined using Cu-K α radiation ($\lambda = 1.5406\text{\AA}$) at 40 kV, and 30 mA. The progressive receiving slit (height 0.30 mm), with a curved graphite monochromator. The intensity data were collected by continuous scanning (step 0.02 $^\circ/\text{s}$) in 2θ angle range of 10 – 80° . The crystalline phase was identified using the International Centre for Diffraction Data (ICDD) database. The Fourier transform infrared the spectrum (FTIR) of magnesium ferrite powders (as pellets in KBr) are recorded with an IR Shimadzu 8400 spectrophotometer over the range of $(400$ – $4000)\text{ cm}^{-1}$. The surface morphology of the obtained samples was inspected by field emission scanning electron

microscopy (FE-SEM) (Model: ZEISS Sigma 300) and "transmission electron microscopy" (TEM) micrographs were obtained utilizing a "JEOL, JEM-2100F" system, the accelerating voltage was 200 kV. To prepare the TEM specimens, powder specimens were distributed in ethanol using the ultrasonic for ten min. A little drop of the specimen solution was dropped on the top surface of a carbon film sustained Cu grid then allowed to dry in the air before the test. For analyzing the composition of the prepared compounds, energy dispersive X-ray spectroscopy (EDX) (ZEISS Sigma 300) was employed. To examine the magnetic properties of the synthesized nano-particles, the magnetization measurements were approved up Saturation using a "vibrating scanning magnetometer (VSM)" (Cryogenic Limited PPMS) under the applied field of ± 1 (T) at room temperature.

3. Results and Discussion

The physical properties of nanomaterials prepared by gel-combustion process are mainly dependent on the type of the used fuel. A wide variety of fuels is used in nanomaterials synthesis by gel-combustion. The sol is developed gradually to the produced of a gel-like network having mix solid and liquid phase at the same time [32]. The homogeneous gel is, then, heated and the auto-combustion has given a good powder. However, preparation of metal oxide includes linking the metal with oxo insides (M-O-M) or hydroxo (M-OH-M) bridges, so producing the metal-oxo or metal-hydroxo polymers in solution.

FTIR spectral analysis

Fig. 1 shows FT-IR spectra for the MgFe_2O_4 samples calcined at 900°C . The dry gel shows an absorption band around 3434 cm^{-1} which corresponding to the bending vibration of N-H. An absorption band around 3305 – 3120 cm^{-1} shown by sample tallies to the presence of O-H group". The strong peaks at 1662 and 1390 cm^{-1} are correspond to bending vibration of carbonyl group and NO_3^- ions, respectively. The absenteeism of absorption bands corresponding to tetrahedral and octahedral complexes specifies that the creation of spinel structure is not complete in the dried gel [33,34].

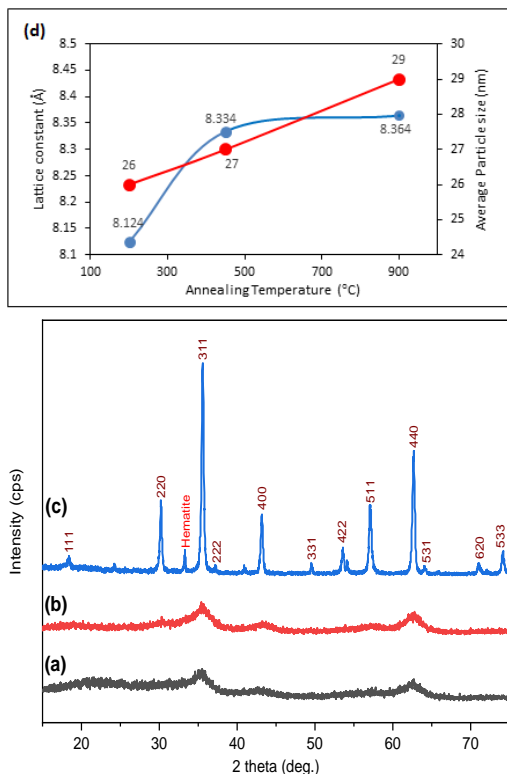


Fig. 2: XRD patterns of magnesium ferrite samples annealed at: (a) 200 °C, (b) 450 °C, and (c) 900 °C. (d) The average particle size and lattice constant for MgFe₂O₄ nanoparticles at the annealing temperature.

Morphological analysis

The morphology of surface and the fundamental structure are investigated by FE-SEM combined with TEM photograph and energy dispersive X-ray analyzes. SEM micrograph and EDX spectrum of MgFe₂O₄ sample calcined at 900°C are shown in Fig. 3a and 3b respectively. It can be perceived that the calcined specimens involve of very tiny particles with a mean particles size nearly 35nm and each particle has a regular shape with a clear glassy nanostructure own polyhedral shapes and very little numbers of circular tiny particles. On the other side, the holes in the micro image are owing to the exit of additional amount of gases throughout the burning method. It is absorbed that the difference in the particle size for the present samples calculated by FE-SEM and the crystallite size obtained using Scherrer’s formula from XRD analysis, may be due to the molecular structural disorder and lattice strain, which results from the different ionic radii and/or clustering of the nanoparticles. Hence, the XRD method has a more stringent criterion and leads to smaller sizes [40]. EDX analysis of the MgFe₂O₄ sample calcined at 900°C is carried out for essential investigation. In the EDX analysis (Fig.3) no pollution element is noticed, excepting magnesium, iron, and oxygen. The atomic fraction of magnesium and iron are about 1:2.

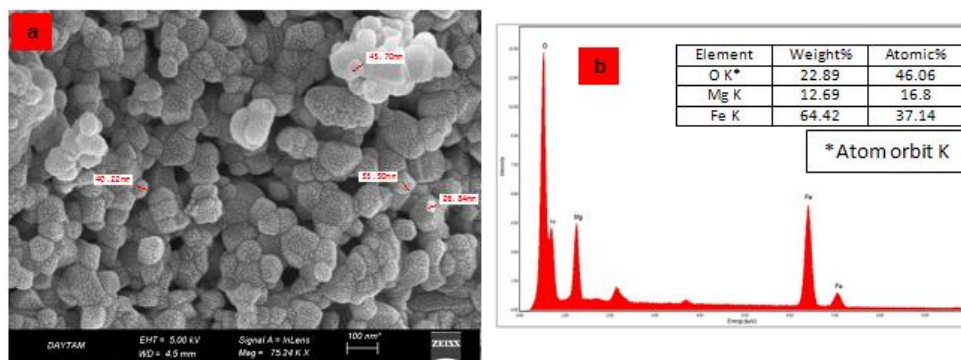


Fig. 3 (a) FE-SEM image and (b) EDX spectra of the MgFe₂O₄ annealed at 900 °C.

Magnetic measurement

The magnetic properties of MgFe₂O₄ can be specified by factors like the grinding process, particles size, cation delivery, and annealing temperature and O² occupancy, etc. The hysteresis curve of the MgFe₂O₄ sample is shown in Fig. 4. The MgFe₂O₄ nanoparticles exhibit the soft ferrimagnetic behavior of the synthesized MgFe₂O₄ and values of the saturation magnetization (*M_s*), remnant magnetization (*M_r*), coercive field (*H_c*) and loop squareness ratio (*M_r/M_s*) are obtained and listed in Table 2. The experimental magnetic moment is meant from the next formulation [34]:

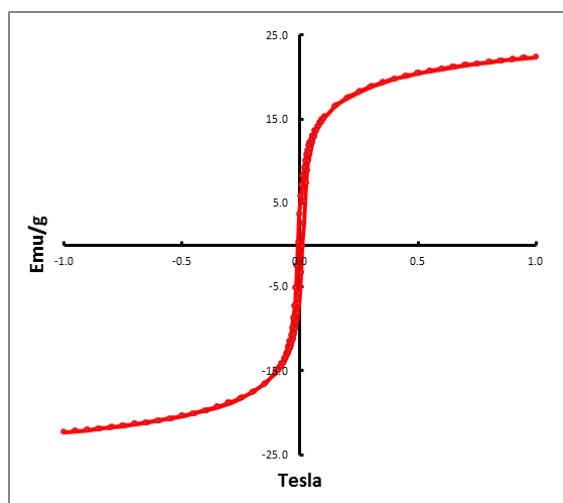
$$\mu_p = MW.M_s / 5585 \dots (3)$$

where MW is the molecular weight of the specimen and M_S is the saturation magnetization in emu/g. Saturation magnetization (*M_s*) of MgFe₂O₄ was 22.4 emu⁻¹ and the high value of the powerful field for

the as-prepared powder of MgFe₂O₄ is confirm to become 104.4 Oe for 29 nm particle size. Several researchers have reported different coercivity values than what we obtained for example, A. Pradeep et al. [34] have determined *H_c* value as 202.55G for 35 nm grain size. Rabanal et al. [41] have determined an *H_c* amount of 576.7 Oe for a grain size of 80 nanometers. A contrast of these values clarifies a straight proportional relation between coercivity and grain size, that is an influence of nano administration where the coercivity of the as-synthesized magnetic nanoparticles is negligible when the nanocrystals have single domains, that refers to much of single domains are regularly magnetized with all the spins aligned in the same direction. This is available only when the particle diameter size below 3–50 nm, depending on the materials.

Table 2. Magnetic parameters extracted from VSM data at room temperature for MgFe₂O₄ annealed at 900 °C

Annealing temp.(°C)	M_s (emu/g)	M_r (emu/g)	H_c (Oe)	M_r/M_s	μ_p
900	22.4	5.87	104.4	0.262	0.802

**Fig. 4 Hysteresis loop of MgFe₂O₄ at room temperature.**

References

- [1] Durrani S. K., Naz S., Mehmood M, Nadeem M. and Siddique M., (2017) "Structural, impedance and Mossbauer studies of magnesium ferrite synthesized via sol-gel auto-combustion process" *Journal of Saudi Chemical Society*. **21** :899-910.
- [2] Kolhatkar A. G., Jamison A. C., Litvinov D., Willson R. C., and Lee T. R., (2013) "Tuning the Magnetic Properties of Nanoparticles" *Int. Journal of Molecular Sciences***14**(8) :15977-16009.
- [3] Vara Prasad B. B. V. S., Ramesh K. V. and Adiraj Srinivas, (2017) "Structural and Magnetic Studies of Nano-crystalline Ferrites MFe₂O₄(M=Zn, Ni, Cu, and Co) Synthesized Via Citrate Gel Autocombustion Method" *Journal of Superconductivity and Novel Magnetism***30** (12): 3523-3535.
- [4] Sharma S., Choudhary N., Verma M. K., Sharma N. D. and Singh D.,(2017) "Cation distribution and magnetic properties of nano and bulk CoCrFeO₄ ferrite synthesized by glycine-nitrate combustion method" *Ceramics International* **43**(14) :11083-11089.
- [5] Reddy C.V.G., Manorama S.V. and Rao V.J., (1999) "Semiconducting gas sensor for chlorine based on inverse spinel nickel ferrite" *Sensors and Actuators B* **55** 90-95.
- [6] Ahmed M.A., Okasha N., and El-Sayed M.M., (2007) " Enhancement of the physical properties of rare-earth-substituted Mn-Zn ferrites prepared by flash method" *Ceramics International* **33**: 49-58.
- [7] Thompson Z., and et.al., (2017) "Fabrication and Characterization of Magnesium Ferrite-Based PCL/Aloe Vera Nanofibers" *Materials* **10**: 2-12.
- [8] Liu Y. L., and et.al., (2005) "Simple synthesis of MgFe₂O₄ nanoparticles as gas sensing materials" *Sensors and Actuators B* **107** :600-604.

4. Conclusion

Nanocrystalline and magnetic spinel MgFe₂O₄ powders are prepared by the sol-gel auto combustion technique using urea as chelating/fuel agents. MgFe₂O₄ showed superparamagnetic behavior after calcination at 900°C for 3h. Analysis of X-ray diffraction pattern confirmed the formation of MgFe₂O₄ as major and minor phases with a small amount of unreacted α - Fe₂O₃. IR analysis presented the characteristic immersion bands and the band sites revealed that divalent cations are dispersed on both positions.

- [9] Dillert R., Taffa D.H., Wark M., Bredow T., and Bahnemann D. W., (2015) "Research update: photoelectrochemical water splitting and photocatalytic hydrogen production using ferrites (MFe₂O₄) under visible light irradiation" *APL Materials*. **3**: 104001.
- [10] Taffa D. H., and et.al., (2017) "Photoelectrochemical and theoretical investigations of spinel type ferrites (M_xFe_{3-x}O₄) for water splitting: A mini-review" *J. Photonics for Energy* **7**: 012009.
- [11] Feng Y., and et.al., (2017) "Preparation and characterization of MgFe₂O₄ nanocrystallites via PVA sol-gel route" *Journal of Alloys and Compounds* **699**: 521-525.
- [12] Hashishin T., and et.al., (2016) "Magnesium ferrite sensor for H₂S detection" *Sensors and Materials* **28**: 1229-1236.
- [13] Babu Reddy L.P., and et.al., (2018) "Role of molybdenum trioxide in enhancing the humidity sensing performance of magnesium ferrite/molybdenum trioxide composite" *Journal of Inorganic Chemistry Communications* **98**: 68-74.
- [14] Rezlescu N., Rezlescu E., Sachelarie L., Popa P.D., and Doroftei C. (2014) "Structural and catalytic properties of mesoporous nanocrystalline mixed oxides containing magnesium" *Catalysis Communications* **46** : 51-56.
- [15] Sivakumar N., and et.al., (2011) "Nanostructured MgFe₂O₄ as anode materials for lithium-ion batteries" *Journal of Alloys and Compounds* **509**: 7038-7041.
- [16] Suharyadi E., Hermawan A., and Puspitarum D. L., (2018) "Crystal Structure and Magnetic Properties of Magnesium Ferrite (MgFe₂O₄) Nanoparticles Synthesized by Coprecipitation Method", *Journal of Physics: Conference Series***109**: 101-2003.

- [17] Patil J.Y., Mulla I.S., and Suryavanshi S.S., (2013) "Gas response properties of citrate gel synthesized nanocrystalline $MgFe_2O_4$: Effect of sintering temperature", *Materials Research Bulletin* **48**: 778-784.
- [18] Kofenstein R., Walther T., Hesse D., and Ebbinghaus S. G., (2013) "Preparation and characterization of nanosized magnesium ferrite powders by a starch-gel process and corresponding ceramics" *Journal of Materials Science* **48**: 6509-6518.
- [19] Hussein S. I., Elkady A. S., Rashad M.M., Mostafa A.G., and Megahid R.M., (2015) "Structural and magnetic properties of magnesium ferrite nanoparticles prepared via EDTA-based sol-gel reaction" *Journal of Magnetism and Magnetic Materials* **379**: 9-15.
- [20] Paulsingh R., and Venkataraju C., (2018) "Effect of calcinations on the structural and magnetic properties of magnesium ferrite nanoparticles prepared by sol gel method" *Chinese Journal of Physics* **56**: 2218-2225.
- [21] Goodarz Naseri M., Bin Saion E., Abbastabar Ahangar H., Hashim M., and Shaari A.H., (2011) "Synthesis and characterization of manganese ferrite nanoparticles by thermal treatment method" *Journal of Magnetism and Magnetic Materials* **323**: 1745-1749.
- [22] Chen Q., Rondinone A. J., Chakoumakos B. C., and Zhang Z., (1999) "Synthesis of superparamagnetic $MgFe_2O_4$ nanoparticles by coprecipitation" *Journal of Magnetism and Magnetic Materials* **194**: 1-7.
- [23] Sasaki T., and et.al., (2010) "Continuous synthesis of fine $MgFe_2O_4$ nanoparticles by supercritical hydrothermal reaction" *Journal of Supercritical Fluids* **53**: 92-94.
- [24] Sepelak V., and et.al., (2006) "Nonequilibrium cation distribution, canted spin arrangement, and enhanced magnetization in nanosized $MgFe_2O_4$ prepared by a one-step mechanochemical route" *Chemistry of Materials* **18**: 3057-3067.
- [25] Das H., and et.al., (2018) "Controlled synthesis of dense $MgFe_2O_4$ nanospheres by ultrasonic spray pyrolysis technique: Effect of ethanol addition to precursor solvent" *Advanced Power Technologies* **29**: 283-288.
- [26] Ghosh S.K., Prakash A., Datta S., Roy S.K. and Basu D., (2010) "Effect of fuel characteristics on synthesis of calcium hydroxyapatite by solution combustion route" *Bulletin of Materials Science* **33**: 7-16
- [27] Ghosh S.K., and et.al., (2008) "In vivo response of porous hydroxyapatite and b-tricalcium phosphate prepared by aqueous solution combustion method and comparison with bioglass scaffolds" *Journal of Biomedical Materials Research Part B*, **86**: 217-227
- [28] Han Y., Li S., Wang X. and Chen X. (2004) "Synthesis and sintering of nanocrystalline hydroxyapatite powders by citric acid sol-gel combustion method" *Materials Research Bulletin*, **39**: 25-32.
- [29] Wang W., Zang C. and Jiao Q., (2014) "Synthesis, structure and electromagnetic properties of Mn-Zn ferrite by sol-gel combustion technique" *Journal of Magnetism and Magnetic Materials*, **349**: 116-120.
- [30] Ayazi Z., Khoshhesab Z. M. and Amani-Ghadim A., (2018) "Synthesis of nickel ferrite nanoparticles as an efficient magnetic sorbent for removal of an azo-dye: Response surface methodology and neural network modeling" *Nanochemistry Research* **3(1)**: 109-123.
- [31] Motlagh M. M., Masoudpanah S. M., Hasheminasari M. and Beigdelou R., (2018) "Effect of solvent's types on the structure and magnetic properties of the as-coprecipitated Fe_3O_4 nanoparticles" *Journal of Ultrafine Grained and Nanostructured Materials* **51**: 163-168.
- [32] Cheruku R., Vijayan L. and Govindaraj G., (2013) "Ion dynamics in sol - gel synthesized $Li_2Ni_{1-x}Mg_xTiO_4$ nanocrystallites" *Materials Chemistry and Physics* **141**: 620-628.
- [33] Huang Y., Tang Y., Wang J. and Chen Q., (2006) "Synthesis of $MgFe_2O_4$ nanocrystallites under mild conditions" *Materials Chemistry and Physics*. **97**: 394-397.
- [34] Pradeep A., Priyadharsini P. and Chandrasekaran G., (2008) "Sol-gel route of synthesis of nanoparticles of $MgFe_2O_4$ and XRD, FTIR and VSM study" *Journal of Magnetism and Magnetic Materials* **320**: 2774-2779.
- [35] Roberto K., Walther T., Hesse D. and Ebbinghaus S.G., (2013) "Preparation and characterization of nanosized magnesium ferrite powders by a starch-gel process and corresponding ceramics" *Journal of Materials Science* **48**: 6509-6518
- [36] Gadkari A.B., Shinde T.J. and Vasambekar P.N., (2010) "Structural and magnetic properties of nanocrystalline Mg-Cd ferrites prepared by oxalate co-precipitation method" *Journal of Materials Science: Materials in Electronics* **21**: 96-103.
- [37] Peddis D., and et.al., (2013) "Beyond the effect of particle size: Influence of $CoFe_2O_4$ nanoparticle arrangements on magnetic properties" *Chemistry of Materials* **25**: 2005-2013.
- [38] Yadav R. S., and et.al., (2017) "Impact of grain size and structural changes on magnetic, dielectric, electrical, impedance and modulus spectroscopic characteristics of $CoFe_2O_4$ nanoparticles synthesized by honey mediated sol-gel combustion method" *Advances in Natural Sciences: Nanoscience and Nanotechnology* **8**: 1-14.
- [39] Dixit G., Singh J. P., Srivastava R.C. and Agrawal H.M., (2012) "Magnetic resonance study of Ce and Gd doped $NiFe_2O_4$ nanoparticles" *Journal of Magnetism and Magnetic Materials*. **324**: 479-483.
- [40] Sujatha C., Reddy K. V., Babu K. S., Reddy A. R. and Rao K., (2012) "Effects of heat treatment

conditions on the structural and magnetic properties of MgCuZn nano ferrite" *Ceramics International* **38** : 5813-5820.

[41] Rabanal M.E., Várez A., Levenfeld B. and Torralba J.M., (2003) "Magnetic properties of Mg-ferrite after milling process" *Journal of Materials Processing Technology* **143-144** : 470-474.

تحضير جسيمات المغنيسيوم فرايت النانوية عن طريق الاحتراق التلقائي وبحث خصائصها الهيكلية والمورفولوجية والمغناطيسية

ابراهيم فهد وحيد ، فائز محسن حامد ، بيداء محمود علي

قسم الكيمياء ، كلية العلوم ، جامعة تكريت ، تكريت ، العراق

الملخص

تم تحضير دقائق المغنيسيوم فرايت النانوية ($MgFe_2O_4$) عن طريق الاحتراق الذاتي للسول-جل والمكلسنة عند 900 درجة مئوية. حيث كانت اليوريا هي العامل الشابك وتترات المغنيسيوم والحديد كمصادر للفلز. أظهر حيود الأشعة السينية (XRD) وطيف (FTIR) الأتماط المميزة لتكوين بنية المكعب. كما أظهر طيف الأشعة تحت الحمراء حزمة ارتباط الأوكسجين بالفلز عند (574-433) و (703-636) cm^{-1} والتي تشير لمواقع رباعي السطوح وثمانى السطوح لنظام المغنيسيوم فرايت. كما تم فحص الصور المأخوذة بمجهر المسح الإلكتروني (SEM) حيث كانت البلورات ذات بنية تركيبية دقيقة واضحة لها أشكال متعددة السطوح وأعداد صغيرة جداً من الجزيئات الكروية الصغيرة. كما تم حساب الحجم البلوري لدقائق المغنيسيوم فرايت النانوية باستخدام معادلة Debye-Scherrer حيث كانت بحدود 29 نانومتر.